

HAVEN: Hierarchical Cooperative Multi-Agent Reinforcement Learning with Dual Coordination Mechanism

Zhiwei Xu, Yunpeng Bai, Bin Zhang, Dapeng Li, Guoliang Fan

Institute of Automation, Chinese Academy of Sciences
School of Artificial Intelligence, University of Chinese Academy of Sciences
Beijing, China

{xuzhiwei2019, baiyunpeng2020, zhangbin2020, lidapeng2020, guoliang.fan}@ia.ac.cn

Abstract

Multi-agent reinforcement learning often suffers from the exponentially larger action space caused by a large number of agents. In this paper, we propose a novel value decomposition framework HAVEN based on hierarchical reinforcement learning for the fully cooperative multi-agent problems. In order to address instabilities that arise from the concurrent optimization of high-level and low-level policies and another concurrent optimization of agents, we introduce the dual coordination mechanism of inter-layer strategies and inter-agent strategies. HAVEN does not require domain knowledge and pretraining at all, and can be applied to any value decomposition variants. Our method is demonstrated to achieve superior results to many baselines on StarCraft II micromanagement tasks and offers an efficient solution to multi-agent hierarchical reinforcement learning in fully cooperative scenarios.

In the last few years there has been a growing interest in multi-agent reinforcement learning (MARL), which plays an vital role in various tasks such as traffic control (Kuyer et al. 2008), recommendation systems (Choi et al. 2018) and game AI (Vinyals et al. 2019). Most of the multi-agent reinforcement learning algorithms follow the paradigm known as centralized training with decentralized execution (CTDE), which means each agent can use all available information during training but only make decisions on the basis of its own observation. According to this principles, MARL algorithms can be divided into several categories including ones based on centralized critics and decentralized actors (Lowe et al. 2017; Foerster et al. 2018; Iqbal and Sha 2019), communication (Sukhbaatar, Szlam, and Fergus 2016; Foerster et al. 2016; Peng et al. 2017), and value decomposition (Sunehag et al. 2018; Rashid et al. 2018; Son et al. 2019). In some cooperation scenarios, the value decomposition methods can significantly alleviate the credit assignment problem. Several value decomposition variants have been proposed and achieved far-reaching performance improvements recently.

However, most of the previous studies on multi-agent cooperative tasks do not take the hierarchical decomposition into account. For example, as the central nervous system, the brain often controls the lower level nervous system instead of directly controlling the muscles to complete specific actions. The hierarchical structure can decompose the action space exponentially related to the number of agents,

thereby reducing computational complexity. Besides, the advantage of the hierarchical approach is its better interpretability. Hierarchical reinforcement learning (HRL) is realized based on the idea that decompose the complex tasks into some simpler subtasks. Traditional hierarchical reinforcement learning methods include hierarchical abstraction machine (HAM) (Parr and Russell 1997), MAXQ (Dietterich 2000), option (Sutton, Precup, and Singh 1999; Precup and Sutton 2000) and feudal neural networks (Dayan and Hinton 1992). With the recent development of deep learning, HRL has gradually gradually developed into two main branches: subgoal-based methods (Vezhnevets et al. 2017; Nachum et al. 2018) and option-based methods (Bacon, Harb, and Precup 2017; Harb et al. 2018). And both of them has been utilized in many single-agent applications. However, HRL may not be practical in all situations. For example: it is difficult to generate subgoals by subgoal-based methods; in option-based approach one option often degenerates into a single primitive action; the setup of intrinsic reward requires domain knowledge; and the concurrent optimization of high-level and low-level policies can easily lead to unstable training process and difficult convergence.

In this paper, we propose a new framework for the multi-agent cooperation problems that can be modelled by Dec-POMDPs, **Hier**archical **V**alue **d**ecomposition (**HAVEN**), a hierarchically structured method combined with the value decomposition methods. HAVEN constructs a two-layer strategy, and uses the advantage function of the high-level policy as part of the intrinsic reward of the low-level policy. In this way, the simultaneous optimization of high-level and low-level policies are guaranteed, which alleviates the training instability that was key limitation of the previous HRL work. There is also no need to pretrain the low-level policies. Simultaneously, because the action space of the high-level policies is preset with maintaining the generality, the training process of the entire framework does not require domain knowledge. Besides, it is worth mentioning that HAVEN can be extended to any value decomposition variant. In summary, HAVEN is an end-to-end and knowledge-free framework.

Our contributions include three aspects:

- We presents the HAVEN framework that builds a dual coordination mechanism of inter-level and inter-agent to solve the Dec-POMDP problems.

- Through visualizing the decision-making process, we proved that the decision space is implicitly divided into multiple subspaces by high-level strategies of HAVEN.
- Empirical evaluations in the StarCraft II micromanagement testbed also demonstrate that our method significantly outperforms previous algorithms.

Related Work

A number of approaches to single-agent HRL have been suggested. One is the approach based on options, which abstracts frequently reused subpolicies into actions of the high-level policy. This approach often causes options to degenerate into primitive actions. A somewhat different approach identifies a set of representations (usually the subset of the state space or the hidden variable space) that make for useful subgoals. That is, the output space of the high-level policy is set to the subgoal space, and the low-level policy outputs the primitive actions depending on the subgoals output by the high-level policy. Although this method is relatively close to the way of human decision-making, it is often difficult to implement because the subgoal space is too large. Of course, we can also speed up the training of reinforcement learning by manually setting subgoals (Rafati and Noelle 2019; Song et al. 2019) or intrinsic rewards (Vezhnevets et al. 2017), but this inevitably introduces domain knowledge. In addition, to solve the instability caused by the simultaneous learning of both two levels’ policies, some methods have been proposed. For example, HAAR (Li et al. 2019) calculates advantage-based auxiliary rewards through on-policy algorithms and CHER (Kreidieh et al. 2019) collaboratively optimizes goal-assignment and goal-achievement policies from a multi-agent perspective.

In recent years, the idea of hierarchical structures has gradually been used in multi-agent reinforcement learning. Feudal Multi-agent Hierarchies (FMH) (Ahilan and Dayan 2019) applies the feudal neural network architecture to the multi-agent environments, but the major drawback of this approach is that it cannot be applied to the fully-cooperative setting, in which all agents optimise a shared reward function. In order to address the sparse and delayed reward in the cooperative multi-agent problem, hierarchical deep multi-agent reinforcement learning with temporal abstraction (Tang et al. 2018) such as hierarchical QMIX and hierarchical communication network was proposed. But its significant limitation is that the high-level action space is set manually. Hierarchical learning with skill discovery (HSD) (Yang, Borovikov, and Zha 2020) makes the skills output by the macro policy more diversified through supervised learning, thereby promoting skill discovery. However, we believe that its independent learning of the low-level policies is still susceptible to credit assignment. RODE (Wang et al. 2021b) explicitly divides the action space by clustering actions. Each action subspace corresponds to a kind of "role". This is a novel idea except for the unneglected cost of clustering. Besides, many multi-agent hierarchical algorithms cannot handle large state-action spaces which is more complex than that of the single-agent tasks.

Inspired by HAAR, HAVEN regards the advantage func-

tion as the intrinsic reward of the low-level policies. The difference from the above algorithm is that we extend this method to the off-policy value decomposition method. Meanwhile, based on the joint optimization of high-level policies, we also set the low-level policies to be joint optimization instead of independent training. To sum up, we designed a new technique called the dual coordination mechanism for the concurrent optimizations of inter-layer policies and inter-agent policies. HAVEN in this paper is implemented using QMIX as the basic algorithm, but other value decomposition methods are equally applicable.

Preliminaries

Dec-POMDPs

A fully cooperative multi-agent problem is usually described as a Dec-POMDP (Oliehoek and Amato 2016), which can be represented by the tuple $G = \langle S, U, A, P, r, Z, O, n, \gamma \rangle$. At each time step, each agent $a \in A := \{1, \dots, n\}$ selects the corresponding action $u^a \in U$ with only having accesses to the partial observation $z^a \in Z$ obtained by $O(s, a) : S \times A \rightarrow Z$, where $s \in S$ is the real state of the environment. The joint action of all agents is defined as $\mathbf{u} \in U \equiv U^n$. The environmental dynamics, also known as the state transition function, is written as $P(s' | s, \mathbf{u}) : S \times U \times S \rightarrow [0, 1]$. Significantly different from other problems is that in Dec-POMDPs, all agents share a reward function: $r(s, \mathbf{u}) : S \times U \rightarrow \mathbb{R}$. γ is the discount factor. The joint value function and joint action-value function are respectively expressed as:

$$V^\pi(s) = \mathbb{E}[R_t | s_t = s],$$

$$Q^\pi(s, \mathbf{u}) = \mathbb{E}[R_t | s_t = s, \mathbf{u}_t = \mathbf{u}],$$

where π represents the joint policies of all agents, and $R_t = \sum_{l=0}^{\infty} \gamma^l r_{t+l}$ is the discount return. The goal of the MARL problem in Dec-POMDP is to maximize the discount return.

Hierarchical Reinforcement Learning

Hierarchical reinforcement learning is a structured framework intended to tackle complex problems by learning to make decisions over different levels of temporal abstraction. Since most of the related work is two levels of hierarchy, this paper focuses on the two-level structures. We call the whole hierarchical system the joint policy π^{joint} , which composed of the high-level policy π^h and the low-level policy π^l . In the option-based hierarchical structures, the action space of the high-level policy π^h is discrete, and a low-level policy π^l will be selected from a finite set of low-level policies. For subgoal generation, the output space of the high-level policy π^h is often continuous, and we need to calculate the intrinsic reward to guide the low-level policy π^l to make decisions rely on the goals generated by π^h . High-level strategies and low-level strategies are often at different time granularities. The simpler form is that π^h runs every k step to determine the low-level policies or the subgoal in the next k step. Another more complicated one is to judge whether the subgoal is reached. If π^l completes the subgoal, π^h makes a new decision and selects the next subgoal. Besides, we can set the termination function which can control whether π^h makes a new decision or not. Because HRL has the characteristics of

hierarchical structure and temporal abstraction, it can often alleviate the problems of inexplicability and reward sparse in reinforcement learning.

Value Decomposition

For multi-agent value decomposition methods such as VDN and QMIX, an important concept for such methods is decentralisability. Specifically, the overall and individual interests in the multi-agent system are consistent. This assumption can be formulated as Individual-Global-Max (IGM) (Son et al. 2019) which assumes that the optimality of each agent is consistent with the optimality of all agents. The equation that describes IGM is as follows:

$$\arg \max_{\mathbf{u}} Q_{tot}(\boldsymbol{\tau}, \mathbf{u}) = \begin{pmatrix} \arg \max_{u^1} Q_1(\tau^1, u^1) \\ \vdots \\ \arg \max_{u^n} Q_n(\tau^n, u^n) \end{pmatrix},$$

where $\boldsymbol{\tau} \in T^n$ represents the joint action-observation histories of all agents, Q_{tot} is global action-value function and Q_a is the individual ones.

The earliest value-based method is Value Decomposition Network (Sunehag et al. 2018), which learns a centralized but decomposable Q_{tot} and represents it as the linear summation of the individual Q_a that condition only on individual observations and actions. The sum Q_{tot} of all individual value functions is given by:

$$Q_{tot}(\boldsymbol{\tau}, \mathbf{u}) = \sum_{a=1}^n Q_a(\tau^a, u^a).$$

And QMIX (Rashid et al. 2018) is a follow-up work of VDN, which estimates Q_{tot} as a nonlinear combination of Q_a through the mixing network and introduces the monotonicity constraint:

$$\frac{\partial Q_{tot}(\boldsymbol{\tau}, \mathbf{u})}{\partial Q_a(\tau^a, u^a)} \geq 0, \quad \forall a \in \{1, \dots, n\}.$$

In addition, many variants of value decomposition have been developed, each focusing on different problems. Obviously, they can all become the basic algorithms under the HAVEN framework proposed by us.

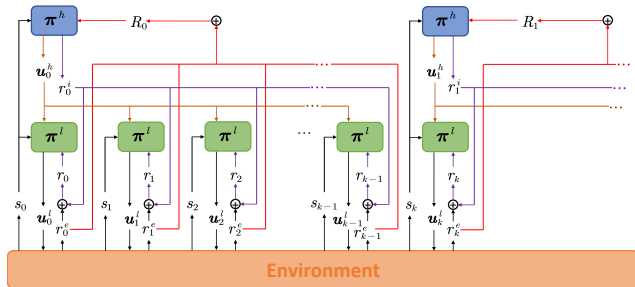


Figure 1: The workflow of HAVEN. The purple lines and the red lines represent the calculation processes of the reward function of π^l and π^h , respectively.

Method

In this section, we introduce the proposed novel hierarchical multi-agent reinforcement learning framework HAVEN. We first describe the entire process of HAVEN interacting with the environment and then elaborate on the specific structure and the implementation. Finally, we give the update functions.

The HAVEN Work Process

Since we are concerned about hierarchical reinforcement learning in the multi-agent environments, to explain concisely, we tend to demonstrate the HAVEN workflow from a perspective similar to single-agent hierarchical reinforcement learning. Each agent a has a high-level policy $\pi^{h,a}$ and a low-level policy $\pi^{l,a}$, and the corresponding action space is the macro action space $u^{h,a} \in U^h$ and the primitive action space $u^{l,a} \in U^l$. In this paper, we define the macro action space U^h as N one-hot variables, so that the output space of $\pi^{h,a}$ is discrete. $\boldsymbol{\pi}^h = \{\pi^{h,1}, \dots, \pi^{h,n}\}$ represents the high-level policies of all agents and $\boldsymbol{\pi}^l = \{\pi^{l,1}, \dots, \pi^{l,n}\}$ denotes the low-level ones. We use this definition to move closer to the general single-agent hierarchical reinforcement learning.

HAVEN use a two-timescale framework, so we define T and t as the time scales of the high-level policy and the low-level policy, respectively. In this work, we make $\boldsymbol{\pi}^h$ to be executed every k steps at a slow timescale. After $\boldsymbol{\pi}^h$ selects the joint macro action \mathbf{u}^h , $\boldsymbol{\pi}^l$ will select the joint primitive action \mathbf{u}^l depending on the real-time state s (available only during training) and the local observation \mathbf{z} for k steps. In Dec-POMDPs, all agents share a reward function given by environments and we denote it as the external reward r^e of $\boldsymbol{\pi}^l$. We also set the high-level reward function to be shared, defined as $R_T = \sum_{i=0}^{k-1} r_{T \cdot k + i}^e$. We denote the replay buffer of the both level policies as \mathcal{D}^l and \mathcal{D}^h respectively, and the stored trajectories correspond to $\langle s_t, \mathbf{z}_t, \mathbf{u}_{[t/k]}^h, \mathbf{u}_t^l, r_t^e \rangle$ and $\langle s_T, \mathbf{z}_T, \mathbf{u}_T^h, R_T \rangle$.

For the sake of the collaborative optimization of inter-layer policies, similar to HAAR, we adopt the advantage function of $\boldsymbol{\pi}^h$ as the intrinsic reward of $\boldsymbol{\pi}^l$. When $\boldsymbol{\pi}^h$ perform the joint action \mathbf{u}_T^h in the state s_T , we set the advantage function of \mathbf{u}_T^h is $A(s_T, \mathbf{u}_T^h)$. Then for $\boldsymbol{\pi}^l$, the advantage function A is evenly divided among k steps to get the intrinsic reward of each step, which can be calculated by the following formula:

$$r_t^i = \frac{A(s_T, \mathbf{u}_T^h)}{k}, \quad T \cdot k \leq t < (T + 1) \cdot k. \quad (1)$$

r^i links the strategies of different layers together, and r^e acts as a joint reward function between all agents. The two respectively represent coordination of the inter-layer policies and the inter-agent policies. Therefore, we get the linear combination of the external reward and the intrinsic reward to obtain the reward function $r = r^e + r^i$ of the low-level joint policy $\boldsymbol{\pi}^l$. The whole workflow of HAVEN is shown in Figure 1. It should be noted that the intrinsic reward is calculated during training, which means that r is recalculated every time after sampling previous transitions from the

replay buffers, so r corresponding to each trajectory is not fixed. The calculation methodology of the intrinsic reward represented by the purple line in Figure 1 is only for the convenience of illustration. Furthermore, the definition and calculation of the advantage function $A(s_T, \mathbf{u}_T^h)$ will be explained later.

The HAVEN Framework

To better address the credit assignment problem in Dec-POMDPs, all layer policies in HAVEN use the value decomposition algorithm including a shared Agent Net and a Mixing Net as the basic algorithm. For the high-level policy, at the step T , each agent a chooses the macro action of the current step $u_T^{h,a} = \varepsilon$ -greedy $\left(Q_a^h(\tau_T^{h,a}, u)\right)$ on the condition of local observation z_T^a and the previous macro action $u_{T-1}^{h,a}$. After all agents select the macro action through the Agent Nets composed of DRQN (Hausknecht and Stone 2015) in this way, the corresponding individual macro action-values will be fused by the Mixing Net to obtain the global macro action-value $Q_{tot}^h(\tau^h, \mathbf{u}^h)$. The specific structure of the Mixing Net changes with the basic value decomposition method. Then again, for the low-level policy we also obtain the joint primitive action \mathbf{u}_t^l and the global low-level action-value function $Q_{tot}^l(\tau^l, \mathbf{u}^l)$ through the value decomposition approach. However, the difference is that the input of the low-level Agent Net contains the macro action $u_T^{h,a}$ given by the high-level Agent Net.

To maintain the generality of implementation, we do not modify the QMIX-style framework of basic algorithms. At time step T , however, the advantage function can be defined according to a common form as:

$$A(s_T, \mathbf{u}_T^h) = \mathbb{E}_{s_{T+1} \sim (\pi^h, \pi^l)} \left[R_T + \gamma V^h(s_{T+1}) - V^h(s_T) \right],$$

where $V^h(\cdot)$ represents the expected return in a certain state, that is, the state value function. Therefore, we need to add an additional neural network structure to estimate this function. Enlightened by VDAC (Su, Adams, and Beling 2021), we again calculate the local state value of all agents and then feed them into the Mixing Net to finally get the global state value function. Similarly, the implementation of the Mixing Net differs depending on the basic value decomposition algorithm. The entire framework of HAVEN is depicted in Figure 2. Note that although two sets of neural networks have been added, the parameters of the entire framework did not increase linearly with the number of agents due to the unique parameter sharing mechanism. Furthermore, because the low-level policy runs at a fast timescale while the high-level policy does at a slower rate, the time complexity is not significantly increased compared with the flat structures.

Loss Functions

HAVEN can realize the simultaneous optimization of the inter-layer policies, which is similar to the monotonic improvement of joint policy in HAAR. But the most obvious difference is that HAVEN we proposed is built on the off-policy methods, so it can achieve higher sample efficiency. What's more, to adapt to multi-agent cases, we also take the

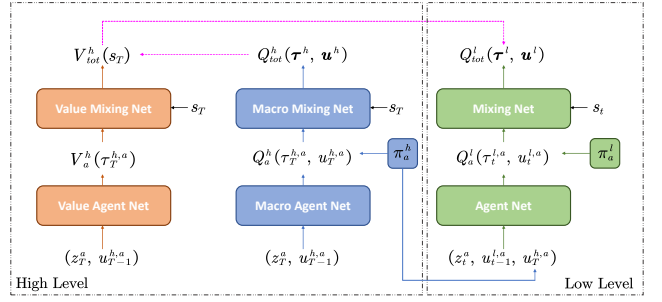


Figure 2: The overall HAVEN architecture. The left part is the high-level policy which includes $V^h(\cdot)$ and $Q^h(\cdot)$ two functions. And the right part is low-level policy which is the vanilla value decomposition architecture. The pink dashed arrows indicate that the update of one function is conditioned on another function.

collaboration of the inter-agent policies into consideration. To accomplish these objectives, we apply the following off-policy update formula of the value function $V^h(\cdot)$:

$$V^h(s_T) = (1 - \alpha)V^h(s_T) + \alpha(R_T + \gamma \max_{\mathbf{u}^h} Q_{tot}^h(\tau_{T+1}^h, \mathbf{u}^h)), \quad (2)$$

where α is the learning rate. Therefore, $V^h(\cdot)$ in the high-level policy is the same as in the QVMAX (Wiering and Hasselt 2009), but the update method of the action-value function $Q^h(\cdot)$ is still consistent with vanilla Q-learning. Through the above changes, we convert the update of $V^h(\cdot)$ to the off-policy method without any modification of $Q^h(\cdot)$ and $Q^l(\cdot)$.

We take the initial state value as the optimization goal, which means we need to find a suitable joint policy π^{joint} to maximize it. Now we can derive $\eta(\pi^{joint})$ according to Eq. (3):

$$\begin{aligned} \eta(\pi^{joint}) &= \mathbb{E}_{s_0^h} \left[V^h(s_0^h) \right] \\ &= \mathbb{E}_{s_0^h, \mathbf{u}_0^h, \dots \sim \pi^{joint}} \left[\sum_T \gamma^T R(s_T^h) \right]. \end{aligned} \quad (3)$$

We can easily get that, in the case of fixed low-level policy π^l , optimizing high-level policy π^h leads to improvement in the joint policy π^{joint} . For the optimization of the low-level policy, we need some proof. Assuming that we optimize the low-level policy when the high-level policy is fixed, use $\tilde{\pi}^{joint}$ and $\tilde{\pi}^l$ to represent the updated joint policy and the low-level policy. According to the proof of HAAR in single-agent cases, we can generalize it to multi-agent situations and obtain the optimization target of $\tilde{\pi}^{joint}$ and $\tilde{\pi}^l$:

$$\begin{aligned} \eta(\tilde{\pi}^{joint}) &\approx \eta(\pi^{joint}) \\ &+ \mathbb{E}_{(s_T^h, \mathbf{u}_T^h) \sim \tilde{\pi}^{joint}} \left[\sum_T \gamma^T A_h(s_T^h, \mathbf{u}_T^h) \right], \end{aligned} \quad (4)$$

$$\begin{aligned} \eta(\tilde{\pi}^l) &\approx \eta(\pi^{joint}) \\ &+ \left[1 + \frac{1 - \gamma_l^k}{k(1 - \gamma_l)} \right] \mathbb{E}_{\tau_h \sim (\tilde{\pi}^l, \pi_h)} \left[\sum_T \gamma_h^T A_h(s_T^h, \mathbf{u}_T^h) \right]. \end{aligned} \quad (5)$$

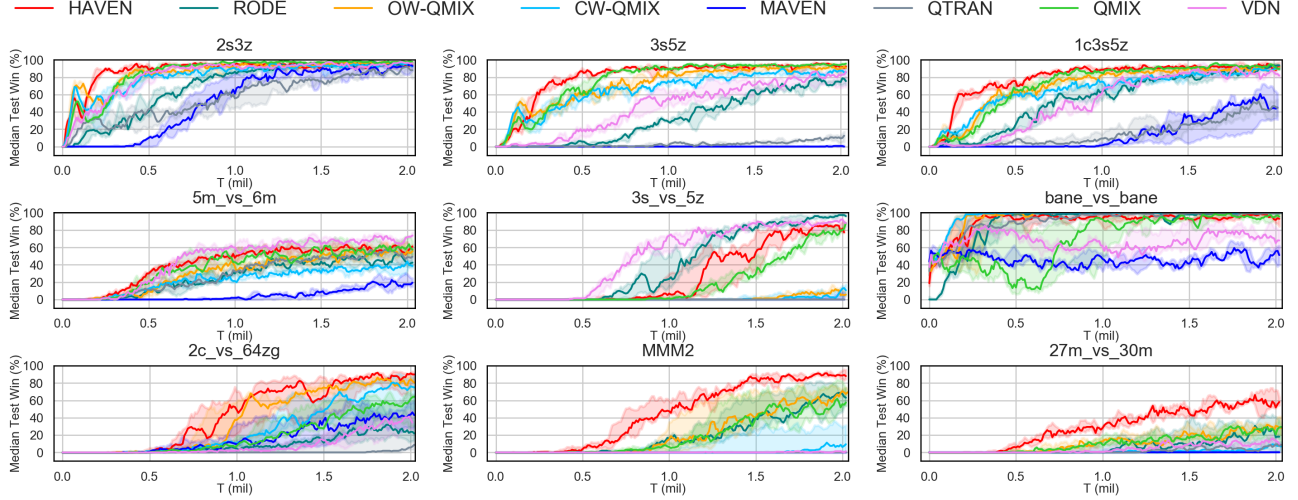


Figure 3: Performance comparison with baselines in different scenarios.

The proof of Eq. (5) can be found in Appendix A. When the two-level discount factors γ_l and γ_h are close to 1 and k is not large, we can get that the optimization goals of the joint policy and the low-level policy have both the term $\mathbb{E}_{\tau_h \sim (\tilde{\pi}^l, \pi^h)} [\sum_T \gamma_h^T A_h(s_T^h, \mathbf{u}_T^h)]$. Meantime, since the updated policy has nothing to do with the original joint policy π^{joint} , the optimization goals of the two can be further simplified:

$$\begin{aligned} \max_{\tilde{\pi}^{joint}} \eta(\tilde{\pi}^{joint}) &= \max_{\tilde{\pi}^{joint}} \mathbb{E}_{(s_t^h, \mathbf{u}_t^h) \sim \tilde{\pi}} \left[\sum_T \gamma_h^T A_h(s_T^h, \mathbf{u}_T^h) \right], \\ \max_{\tilde{\pi}^l} \eta(\tilde{\pi}^l) &= \\ \max_{\tilde{\pi}^l} \left[1 + \frac{1 - \gamma_l^k}{k(1 - \gamma_l)} \right] &\mathbb{E}_{\tau_h \sim (\tilde{\pi}^l, \pi^h)} \left[\sum_T \gamma_h^T A_h(s_T^h, \mathbf{u}_T^h) \right]. \end{aligned}$$

$1 + \frac{1 - \gamma_l^k}{k(1 - \gamma_l)}$ is obviously a positive value, so when we maximize Eq. (5), $\eta(\tilde{\pi}^{joint})$ in Eq. (4) also increases. That is to say, when we monotonically optimize the high-level policy π^h and the low-level policy π^l , the joint policy π^{joint} is also monotonically optimized. So the above updating scheme of hierarchical structures avoids instability of the concurrent optimization of inter-level policies. Meanwhile, It's worth noting that the reward function of π^l includes two parts: intrinsic reward r^i and external reward r^e . External rewards can improve cooperation between agents through the value decomposition mechanism of the low-level policy.

From the above explanation, we can get the loss function of the three sets of neural networks: the high-level state value network, the high-level action-value network and the bottom-level action-value network. θ , ϕ , and ψ represent their parameters, respectively. Thus, the following loss func-

tion is obtained:

$$\begin{aligned} \mathcal{L}_Q^h(\theta) &= \\ \left(R + \gamma_h \max_{\mathbf{u}^{h'}} Q_{tot}^h(\tau^{h'}, \mathbf{u}^{h'} | \theta^-) - Q_{tot}^h(\tau^h, \mathbf{u}^h | \theta) \right)^2, \\ \mathcal{L}_V^h(\phi) &= \left(R + \gamma_h \max_{\mathbf{u}^{h'}} Q_{tot}^h(\tau^{h'}, \mathbf{u}^{h'} | \theta) - V^h(s) \right)^2, \\ \mathcal{L}_Q^l(\psi) &= \\ \left(r + \gamma_l \max_{\mathbf{u}^{l'}} Q_{tot}^l(\tau^{l'}, \mathbf{u}^{l'} | \psi^-) - Q_{tot}^l(\tau^l, \mathbf{u}^l | \psi) \right)^2, \end{aligned}$$

where θ^- and ψ^- refer to the parameters of the high-level and low-level action-value target network respectively. It is worth mentioning that the optimization of the three networks are independent of each other. And in the previous proof it is assumed that the high-level policy and the low-level policy are optimized in turn, either optimizing π^h or optimizing π^l . But in order to improve the sample efficiency, we optimize both of them simultaneously in the actual framework implementation. Experiments show that by optimizing the two-layer policies simultaneously, HAVEN can still greatly outperform other baselines.

Experiments

In this section, we test our method on the StarCraft II micromangement benchmark. Then by carrying out ablation studies, we show that each module that constitutes HAVEN is not redundant. We also investigate the influence of different hyperparameter settings. Finally, we make the visualization of high-level policies, which sheds further light on the capacity of HAVEN to implicitly divide the decision space.

Setup

We first evaluate the performance of HAVEN in the SMAC testbed and compare it with other popular baselines. SMAC is a multi-agent reinforcement learning environment based

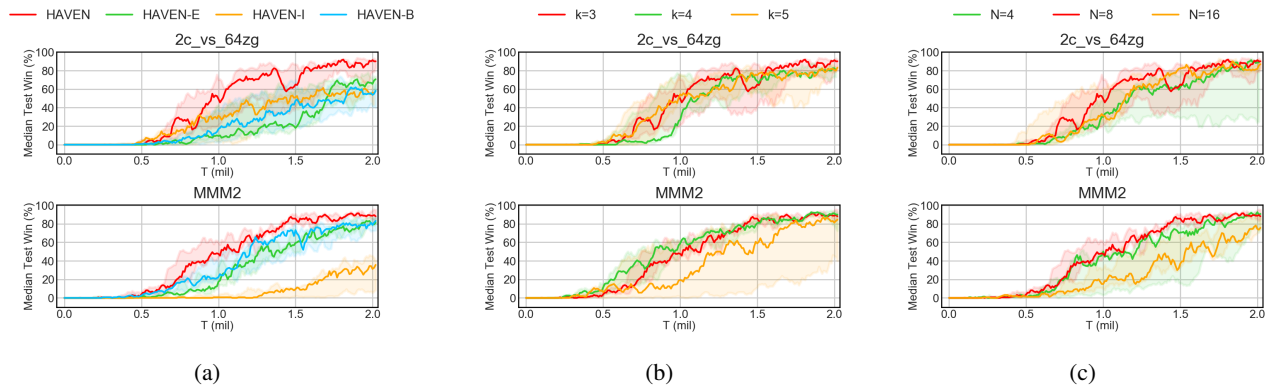


Figure 4: (a) Win rates for HAVEN and ablations. (b) Influence of the k for HAVEN. (c) HAVEN with different N values.

on the real-time strategy game StarCraft II. It contains a wealth of Dec-POMDP micromanagement tasks. Different tasks correspond to different difficulties and different multi-agent cooperation problems, including heterogeneity, large action space, asymmetry and so on. In order to verify the validity of our method, We choose the most common method QMIX as the basic algorithm of HAVEN. Of course, HAVEN can also be built based on other value decomposition algorithms.

The implementation of HAVEN and other benchmarks in our experiment are based on Pymarl. To make the empirical results more convincing, we compare with some state-of-the-art value decomposition approaches including VDN (Su, Adams, and Beling 2021), QMIX (Rashid et al. 2018), QTRAN (Son et al. 2019), Weighted QMIX (Rashid et al. 2020), MAVEN (Mahajan et al. 2019) and RODE (Wang et al. 2021b). We set the hyperparameters of the basic algorithm in HAVEN and those of other baseline algorithms as default. For HAVEN’s unique hyperparameters k and N we set to 3 and 8, respectively. Besides, we also carry out some ablation studies and discuss the influence of different values of k and N . The ablation experiments include setting the reward function of the low-level policies to (1) only the intrinsic reward r^i or (2) only the external reward r^e , and (3) the update formula of the value function $V^h(\cdot)$ does not use the Eq. (2) but uses the general bootstrap update formula which is described by Eq. (6):

$$V(s_T) = V(s_T) + \alpha(R_T + \gamma V(s_{T+1}) - V(s_T)). \quad (6)$$

The above three alterations of HAVEN are called HAVEN-I, HAVEN-E and HAVEN-B respectively. Recall that the high-level policy is executed every k timesteps and the number of macro actions is N . For the k and N , we choose different values of the two to explore how they influence the performance. We run all experiments independently for evaluation with five different random seeds. The version of StarCraft II is SC2.4.6.2.69232 which is the same version as (Rashid et al. 2018, 2020), not the newer SC2.4.10.

Results

In Figure 3, we show the performance comparison between HAVEN based on QMIX and other baselines in different scenarios. The solid lines represent the median win rates, and the 25-75% percentiles are shaded. According to the different difficult levels, the tasks in SMAC can be divided into three types: easy ($2s3z$, $3s5z$ and $1c3s5z$), hard ($5m_vs_6m$, $3s_vs_5z$, $bane_vs_bane$ and $2c_vs_64zg$) and super hard ($MMM2$ and $27m_vs_30m$) scenarios. The performance of our method is significantly better than its basic algorithm QMIX and many other algorithms. The superiority of HAVEN is more obvious in hard scenario $2c_vs_64zg$ and super hard scenarios $MMM2$ and $27m_vs_30m$. The reason for this phenomenon may be due to the large number of agents or the large action space in these scenarios. The flat structure often requires more trajectories to explore the entire decision space. And because HAVEN has a hierarchical structure with coordination of inter-level policies, high-level policies can effectively divide the entire decision space into few smaller ones. In this way, the low-level policy can operate in relatively small decision space. In some easy scenarios, HAVEN can still maintain a higher learning speed than other baselines, which is difficult for some other more complex value decomposition methods. In addition to QMIX, we believe that HAVEN based on other value decomposition methods such like QPLEX (Wang et al. 2021a) has greater potential.

We carry out ablation experiments on two typical scenarios $2c_vs_64zg$ and $MMM2$, which correspond to the problems of the large decision space, to test three main contributions in HAVEN: (1) the intrinsic reward of the low-level policy; (2) the external reward of the low-level policy; (3) The non-bootstrapping and off-policy update mode of the value network. HAVEN-I, HAVEN-E, and HAVEN-B respectively correspond to the ablations in which one of the above three is different from the original HAVEN while the other parts remain unchanged. From Figure 4(a) it can be seen that no matter which ablations, its performance is significantly worse than that of original HAVEN. Especially in scenario $MMM2$, the performance of HAVEN-I that only contains the intrinsic reward for the low-level policy is

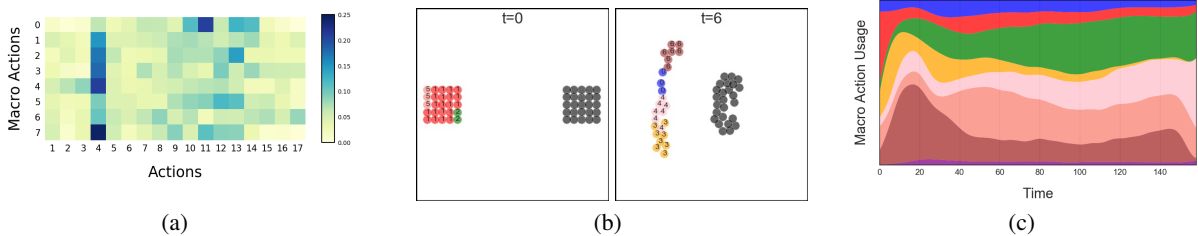


Figure 5: Visualization of high-level policies. (a) Distribution of primitive actions for each macro action. (b) Two game snapshots in one episode on $25m$ scenario. Gray dots are the enemies and color dots are allies. Different color corresponding to different macro actions. (c) Stream graph of macro action usage in one episode on $25m$ scenario.

far worse than other ablations and the original framework, which means that it is not enough to only achieve coordination between different layers in some scenarios. As mentioned above, these three contributions are meaningful to improve the performance of HAVEN.

Finally, in Figure 4(b) and Figure 4(c), we show the influence of various hyperparameter settings on the performance of HAVEN. Similar to the ablation studies, we also choose $2c_vs_64zg$ and $MMM2$ two scenarios for testing. First, we focus on the k which decides how frequently the low-level action spaces change and discuss how the k influences the performance. The results show a trend that HAVEN performs worse as the k is larger, and this phenomenon is more pronounced in $MMM2$. The experimental results match the assumption made in the previous section: k cannot be very large. Regarding the setting of the number of macro actions N , we found that neither too large nor too little will work. Too few macro actions will lead to incomplete division of the decision space and slow down the learning speed of low-level policies; conversely, too many macro actions will increase the decision space of high-level policies in a disguised form and hinder the learning of high-level policies. Therefore, it is necessary to set a relatively reasonable hyperparameter N for the number of macro actions.

In short, HAVEN can implicitly divide the decision space of the original problem. When it can balance the division of the high-level and low-level action space, HAVEN can get amazing performance results. Meantime, HAVEN benefits from the dual coordination mechanism of inter-level policies and inter-agent policies, which is also one of the important reasons for its outstanding performance.

Visualization of High-level Policies

We visualize the high-level policy on specific maps to more intuitively depict the idea of dividing the decision space. We elaborate from three aspects on that: (1) the occurrence of the macro actions and the primitive actions, (2) the relationship between the macro action usage and the positions of the agents, and (3) the dynamic changes of the macro action usage in different time periods.

First, Figure 5(a) shows the distribution of each primitive action when conditioned on each macro action. Since the primitive action 0 that represents the action only taken by the dead agents is meaningless, we don't care about it.

We can clearly see that the distribution corresponding to each macro action is significantly different from each other, which means that the high-level strategies in HAVEN are distinguishable and do not degenerate into one macro action.

The relationship between the macro action usage and the positions of the agents is depicted in Figure 5(b). We depict one-to-one scatter diagram of the positions and the macro actions at two different timesteps in one episode on scenario $25m$ which presents a massive Multi-Agent task. Adjacent agents often choose the same macro actions, which is consistent with the practical multi-agent system. This is very similar to the role division in RODE, except that the division of macro actions in HAVEN is end-to-end and does not utilize the hard mask. And our method does not need pre-training at all.

The dynamic changes of high-level strategies over time can also reflect the division of decision space. In different stages of one episode, different macro actions will always dominate all other macro actions. We use the frequency to represent this dominance, as shown in Figure 5(c). This phenomenon suggests that the agent can find the optimal solution in different decision subspaces at different time periods.

Conclusion

In this paper, we propose a novel hierarchical value decomposition framework HAVEN, which is simple yet so effective and can be applied to any value decomposition variants. Through the hierarchical structure, HAVEN can implicitly decompose the original huge decision space of the multi-agent system. The dual coordination mechanism for the simultaneous learning of inter-level policies and inter-agent policies also provides a solid theoretical foundation for the excellent performance of HAVEN. Therefore, HAVEN does not need to manually set high-level decision spaces and carry out pretraining. The experimental results show that HAVEN can effectively improve the performance of basic algorithms, no matter in simple or difficult scenarios. We believe that our proposed HAVEN framework provides a stable and efficient approach for multi-agent hierarchical reinforcement learning.

In our future research we intend to concentrate on the multi-layer decision structures rather than the simple two-layer structures. Besides, how to select the number of actions for high-level policies and whether the trained low-

level policies can be transferred to other tasks are also valuable extensions. Further study of the issues would be of interest.

References

- Ahilan, S.; and Dayan, P. 2019. Feudal Multi-Agent Hierarchies for Cooperative Reinforcement Learning. *ArXiv*, abs/1901.08492.
- Bacon, P.; Harb, J.; and Precup, D. 2017. The Option-Critic Architecture. In Singh, S. P.; and Markovitch, S., eds., *Proceedings of the Thirty-First AAAI Conference on Artificial Intelligence, February 4-9, 2017, San Francisco, California, USA*, 1726–1734. AAAI Press.
- Choi, S.; Ha, H.; Hwang, U.; Kim, C.; Ha, J.-W.; and Yoon, S. 2018. Reinforcement Learning based Recommender System using Biclustering Technique. *ArXiv*, abs/1801.05532.
- Dayan, P.; and Hinton, G. E. 1992. Feudal Reinforcement Learning. In *NIPS*.
- Dietterich, T. G. 2000. Hierarchical Reinforcement Learning with the MAXQ Value Function Decomposition. *ArXiv*, cs.LG/9905014.
- Foerster, J. N.; Assael, Y. M.; de Freitas, N.; and Whiteson, S. 2016. Learning to Communicate with Deep Multi-Agent Reinforcement Learning. In Lee, D. D.; Sugiyama, M.; von Luxburg, U.; Guyon, I.; and Garnett, R., eds., *Advances in Neural Information Processing Systems 29: Annual Conference on Neural Information Processing Systems 2016, December 5-10, 2016, Barcelona, Spain*, 2137–2145.
- Foerster, J. N.; Farquhar, G.; Afouras, T.; Nardelli, N.; and Whiteson, S. 2018. Counterfactual Multi-Agent Policy Gradients. In McIlraith, S. A.; and Weinberger, K. Q., eds., *Proceedings of the Thirty-Second AAAI Conference on Artificial Intelligence, (AAAI-18), the 30th innovative Applications of Artificial Intelligence (IAAI-18), and the 8th AAAI Symposium on Educational Advances in Artificial Intelligence (EAAI-18), New Orleans, Louisiana, USA, February 2-7, 2018*, 2974–2982. AAAI Press.
- Harb, J.; Bacon, P.; Klissarov, M.; and Precup, D. 2018. When Waiting Is Not an Option: Learning Options With a Deliberation Cost. In McIlraith, S. A.; and Weinberger, K. Q., eds., *Proceedings of the Thirty-Second AAAI Conference on Artificial Intelligence, (AAAI-18), the 30th innovative Applications of Artificial Intelligence (IAAI-18), and the 8th AAAI Symposium on Educational Advances in Artificial Intelligence (EAAI-18), New Orleans, Louisiana, USA, February 2-7, 2018*, 3165–3172. AAAI Press.
- Hausknecht, M.; and Stone, P. 2015. Deep Recurrent Q-Learning for Partially Observable MDPs. In *AAAI Fall Symposia*.
- Iqbal, S.; and Sha, F. 2019. Actor-Attention-Critic for Multi-Agent Reinforcement Learning. In Chaudhuri, K.; and Salakhutdinov, R., eds., *Proceedings of the 36th International Conference on Machine Learning, ICML 2019, 9-15 June 2019, Long Beach, California, USA*, volume 97 of *Proceedings of Machine Learning Research*, 2961–2970. PMLR.
- Kreidieh, A. R.; Parajuli, S.; Lichtlé, N.; You, Y.; Nasr, R.; and Bayen, A. 2019. Inter-Level Cooperation in Hierarchical Reinforcement Learning. *ArXiv*, abs/1912.02368.
- Kuyer, L.; Whiteson, S.; Bakker, B.; and Vlassis, N. 2008. Multiagent Reinforcement Learning for Urban Traffic Control Using Coordination Graphs. In *ECML/PKDD*.
- Li, S.; Wang, R.; Tang, M.; and Zhang, C. 2019. Hierarchical Reinforcement Learning with Advantage-Based Auxiliary Rewards. In Wallach, H. M.; Larochelle, H.; Beygelzimer, A.; d’Alché-Buc, F.; Fox, E. B.; and Garnett, R., eds., *Advances in Neural Information Processing Systems 32: Annual Conference on Neural Information Processing Systems 2019, NeurIPS 2019, December 8-14, 2019, Vancouver, BC, Canada*, 1407–1417.
- Lowe, R.; Wu, Y.; Tamar, A.; Harb, J.; Abbeel, P.; and Mordatch, I. 2017. Multi-Agent Actor-Critic for Mixed Cooperative-Competitive Environments. In Guyon, I.; von Luxburg, U.; Bengio, S.; Wallach, H. M.; Fergus, R.; Vishwanathan, S. V. N.; and Garnett, R., eds., *Advances in Neural Information Processing Systems 30: Annual Conference on Neural Information Processing Systems 2017, December 4-9, 2017, Long Beach, CA, USA*, 6379–6390.
- Mahajan, A.; Rashid, T.; Samvelyan, M.; and Whiteson, S. 2019. MAVEN: Multi-Agent Variational Exploration. In Wallach, H. M.; Larochelle, H.; Beygelzimer, A.; d’Alché-Buc, F.; Fox, E. B.; and Garnett, R., eds., *Advances in Neural Information Processing Systems 32: Annual Conference on Neural Information Processing Systems 2019, NeurIPS 2019, December 8-14, 2019, Vancouver, BC, Canada*, 7611–7622.
- Nachum, O.; Gu, S.; Lee, H.; and Levine, S. 2018. Data-Efficient Hierarchical Reinforcement Learning. In Bengio, S.; Wallach, H. M.; Larochelle, H.; Grauman, K.; Cesa-Bianchi, N.; and Garnett, R., eds., *Advances in Neural Information Processing Systems 31: Annual Conference on Neural Information Processing Systems 2018, NeurIPS 2018, December 3-8, 2018, Montréal, Canada*, 3307–3317.
- Oliehoek, F.; and Amato, C. 2016. A Concise Introduction to Decentralized POMDPs. In *SpringerBriefs in Intelligent Systems*.
- Parr, R. E.; and Russell, S. J. 1997. Reinforcement Learning with Hierarchies of Machines. In *NIPS*.
- Peng, P.; Wen, Y.; Yang, Y.; Yuan, Q.; Tang, Z.; Long, H.; and Wang, J. 2017. Multiagent Bidirectionally-Coordinated Nets: Emergence of Human-level Coordination in Learning to Play StarCraft Combat Games. *arXiv: Artificial Intelligence*.
- Precup, D.; and Sutton, R. 2000. Temporal abstraction in reinforcement learning. In *ICML 2000*.
- Rafati, J.; and Noelle, D. C. 2019. Learning Representations in Model-Free Hierarchical Reinforcement Learning. In *The Thirty-Third AAAI Conference on Artificial Intelligence, AAAI 2019, The Thirty-First Innovative Applications of Artificial Intelligence Conference, IAAI 2019, The Ninth AAAI Symposium on Educational Advances in Artificial Intelligence, EAAI 2019, Honolulu, Hawaii, USA, January 27 - February 1, 2019*, 10009–10010. AAAI Press.

- Rashid, T.; Farquhar, G.; Peng, B.; and Whiteson, S. 2020. Weighted QMIX: Expanding Monotonic Value Function Factorisation for Deep Multi-Agent Reinforcement Learning. *arXiv: Learning*.
- Rashid, T.; Samvelyan, M.; de Witt, C. S.; Farquhar, G.; Foerster, J. N.; and Whiteson, S. 2018. QMIX: Monotonic Value Function Factorisation for Deep Multi-Agent Reinforcement Learning. In Dy, J. G.; and Krause, A., eds., *Proceedings of the 35th International Conference on Machine Learning, ICML 2018, Stockholmsmässan, Stockholm, Sweden, July 10-15, 2018*, volume 80 of *Proceedings of Machine Learning Research*, 4292–4301. PMLR.
- Son, K.; Kim, D.; Kang, W. J.; Hostallero, D.; and Yi, Y. 2019. QTRAN: Learning to Factorize with Transformation for Cooperative Multi-Agent Reinforcement Learning. In Chaudhuri, K.; and Salakhutdinov, R., eds., *Proceedings of the 36th International Conference on Machine Learning, ICML 2019, 9-15 June 2019, Long Beach, California, USA*, volume 97 of *Proceedings of Machine Learning Research*, 5887–5896. PMLR.
- Song, S.; Weng, J.; Su, H.; Yan, D.; Zou, H.; and Zhu, J. 2019. Playing FPS Games With Environment-Aware Hierarchical Reinforcement Learning. In Kraus, S., ed., *Proceedings of the Twenty-Eighth International Joint Conference on Artificial Intelligence, IJCAI 2019, Macao, China, August 10-16, 2019*, 3475–3482. ijcai.org.
- Su, J.; Adams, S. C.; and Beling, P. 2021. Value-Decomposition Multi-Agent Actor-Critics. In *AAAI*.
- Sukhbaatar, S.; Szlam, A.; and Fergus, R. 2016. Learning Multiagent Communication with Backpropagation. In Lee, D. D.; Sugiyama, M.; von Luxburg, U.; Guyon, I.; and Garnett, R., eds., *Advances in Neural Information Processing Systems 29: Annual Conference on Neural Information Processing Systems 2016, December 5-10, 2016, Barcelona, Spain*, 2244–2252.
- Sunehag, P.; Lever, G.; Gruslys, A.; Czarnecki, W.; Zambaldi, V.; Jaderberg, M.; Lanctot, M.; Sonnerat, N.; Leibo, J. Z.; Tuyls, K.; and Graepel, T. 2018. Value-Decomposition Networks For Cooperative Multi-Agent Learning. *ArXiv*, abs/1706.05296.
- Sutton, R.; Precup, D.; and Singh, S. 1999. Between MDPs and Semi-MDPs: A Framework for Temporal Abstraction in Reinforcement Learning. *Artif. Intell.*, 112: 181–211.
- Tang, H.; Hao, J.; Lv, T.; Chen, Y.; Zhang, Z.; Jia, H.; Ren, C.; Zheng, Y.; Meng, Z.; Fan, C.; and Wang, L. 2018. Hierarchical Deep Multiagent Reinforcement Learning with Temporal Abstraction. *arXiv: Learning*.
- Vezhnevets, A. S.; Osindero, S.; Schaul, T.; Heess, N.; Jaderberg, M.; Silver, D.; and Kavukcuoglu, K. 2017. FeUdal Networks for Hierarchical Reinforcement Learning. In Precup, D.; and Teh, Y. W., eds., *Proceedings of the 34th International Conference on Machine Learning, ICML 2017, Sydney, NSW, Australia, 6-11 August 2017*, volume 70 of *Proceedings of Machine Learning Research*, 3540–3549. PMLR.
- Vinyals, O.; Babuschkin, I.; Czarnecki, W.; Mathieu, M.; Dudzik, A.; Chung, J.; Choi, D. H.; Powell, R.; Ewalds, T.; Georgiev, P.; Oh, J.; Horgan, D.; Kroiss, M.; Danihelka, I.; Huang, A.; Sifre, L.; Cai, T.; Agapiou, J.; Jaderberg, M.; Vezhnevets, A.; Leblond, R.; Pohlen, T.; Dalibard, V.; Budden, D.; Sulsky, Y.; Molloy, J.; Paine, T.; Gulcehre, C.; Wang, Z.; Pfaff, T.; Wu, Y.; Ring, R.; Yogatama, D.; Wünsch, D.; McKinney, K.; Smith, O.; Schaul, T.; Lillicrap, T.; Kavukcuoglu, K.; Hassabis, D.; Apps, C.; and Silver, D. 2019. Grandmaster level in StarCraft II using multi-agent reinforcement learning. *Nature*, 1–5.
- Wang, J.; Ren, Z.; Liu, T.; Yu, Y.; and Zhang, C. 2021a. QPLEX: Duplex Dueling Multi-Agent Q-Learning. *ArXiv*, abs/2008.01062.
- Wang, T.; Gupta, T.; Mahajan, A.; Peng, B.; Whiteson, S.; and Zhang, C. 2021b. RODE: Learning Roles to Decompose Multi-Agent Tasks. *ArXiv*, abs/2010.01523.
- Wiering, M.; and Hasselt, H. V. 2009. The QV family compared to other reinforcement learning algorithms. *2009 IEEE Symposium on Adaptive Dynamic Programming and Reinforcement Learning*, 101–108.
- Yang, J.; Borovikov, I.; and Zha, H. 2020. Hierarchical Cooperative Multi-Agent Reinforcement Learning with Skill Discovery. In *AAMAS*.

A Proof of Eq. (5)

We give out the proof of the optimization target of low-level policies π^l as below:

$$\begin{aligned}
 \eta(\tilde{\pi}^l) &= \mathbb{E}_{s_0^l} [V^l(s_0^l)] \\
 &= \mathbb{E}_{\tau \sim (\tilde{\pi}^l, \pi^h)} \left[\sum_{t=0,1,2,\dots} \gamma_l^t r^l(s_t^l, \mathbf{u}_t^l) \right] \\
 &= \mathbb{E}_{\tau \sim (\tilde{\pi}^l, \pi^h)} \left[\sum_{t=0,k,2k,\dots} \mathbb{E}_{\tau_l(t) \sim (\tilde{\pi}^l, \pi^h)} \left[\sum_{i=0}^{k-1} \gamma_l^{t+i} \left(\frac{1}{k} A_h(s_t^h, \mathbf{u}_t^h) + r^e(s_{t+i}^l, \mathbf{u}_{t+i}^l) \right) \right] \right] \tag{A.1}
 \end{aligned}$$

$$\begin{aligned}
 &= \mathbb{E}_{\tau_h \sim (\tilde{\pi}^l, \pi^h)} \left[\sum_{T=0,1,2,\dots} \sum_{i=0}^{k-1} \gamma_l^{T \cdot k + i} \left(\frac{1}{k} A_h(s_T^h, \mathbf{u}_T^h) \right) \right] \\
 &\quad + \mathbb{E}_{\tau_h \sim (\tilde{\pi}^l, \pi^h)} \left[\sum_{t=0,k,2k,\dots} \mathbb{E}_{\tau_l(t) \sim (\tilde{\pi}^l, \pi^h)} \left[\sum_{i=0}^{k-1} \gamma_l^{t+i} r^e(s_{t+i}^l, \mathbf{u}_{t+i}^l) \right] \right] \tag{A.2}
 \end{aligned}$$

$$\approx \frac{1}{k} \mathbb{E}_{\tau_h \sim (\tilde{\pi}^l, \pi^h)} \left[\sum_{T=0,1,2,\dots} \gamma_l^{T \cdot k} \frac{1 - \gamma_l^k}{1 - \gamma_l} A_h(s_T^h, \mathbf{u}_T^h) \right] + \mathbb{E}_{\tau_h \sim (\tilde{\pi}^l, \pi^h)} \left[\sum_{T=0,1,2,\dots} \gamma_h^T R(s_T^h, \mathbf{u}_T^h) \right] \tag{A.3}$$

$$\approx \frac{1 - \gamma_l^k}{k(1 - \gamma_l)} \mathbb{E}_{\tau_h \sim (\tilde{\pi}^l, \pi^h)} \left[\sum_{T=0,1,2,\dots} \gamma_l^{T \cdot k} A_h(s_T^h, \mathbf{u}_T^h) \right] + \eta(\tilde{\pi}^{joint}) \tag{A.4}$$

$$\begin{aligned}
 &\approx \frac{1 - \gamma_l^k}{k(1 - \gamma_l)} \mathbb{E}_{\tau_h \sim (\tilde{\pi}^l, \pi^h)} \left[\sum_{T=0,1,2,\dots} \gamma_h^T A_h(s_T^h, \mathbf{u}_T^h) \right] + \eta(\pi^{joint}) \\
 &\quad + \mathbb{E}_{\tau_h \sim (\tilde{\pi}^l, \pi^h)} \left[\sum_{T=0,1,2,\dots} \gamma_h^T A_h(s_T^h, \mathbf{u}_T^h) \right] \tag{A.5}
 \end{aligned}$$

$$= \left[1 + \frac{1 - \gamma_l^k}{k(1 - \gamma_l)} \right] \mathbb{E}_{\tau_h \sim (\tilde{\pi}^l, \pi^h)} \left[\sum_{T=0,1,2,\dots} \gamma_h^T A_h(s_T^h, \mathbf{u}_T^h) \right] + \eta(\pi^{joint})$$

The last term in Eq. (A.1) is derived from the definition of the low-level reward function $r = r^i + r^e$. We regard $\sum_{t=0,k,2k,\dots} \mathbb{E}_{\tau_l(t) \sim (\tilde{\pi}^l, \pi^h)} \left[\sum_{i=0}^{k-1} \gamma_l^{t+i} r^e(s_{t+i}^l, \mathbf{u}_{t+i}^l) \right]$ and $\sum_{T=0,1,2,\dots} \gamma_h^T R(s_T^h, \mathbf{u}_T^h)$ as equal under the condition of that γ^l as well as γ^h are both close to 1 and the k is not extremely large. Then Eq. (A.2) can be written as Eq. (A.3) by following the above assumption. Substituting Eq. (3) into Eq. (A.3) yields Eq. (A.4) which is only with reference to π^h . Finally, we replace the optimization target of updated joint policies $\tilde{\pi}^{joint}$ by Eq. (4) and get the last form of the optimization target of π^l .

B Experiment Detail

B.1 StarCraft II Micromanagement Tasks

Depending on the complexity of the scenarios, the duration of each experiment ranges from 6 to 14 hours. The detailed information of all scenarios is summarized in the Table B.1. Since the difficulty of the map is determined based on version 4.6.2.69232 of StarCraft II, we carried out all experiments on StarCraft II of this relatively more difficult version instead of version 4.10. The results of some benchmarks in this paper are different from those in the literature, which may be caused by inconsistent versions of StarCraft II.

Name	Ally Units	Enemy Units	Type	Difficulty
2s3z	2 Stalkers	2 Stalkers	Heterogeneous	Easy
	3 Zealots	3 Zealots	Symmetric	
3s5z	3 Stalkers	3 Stalkers	Heterogeneous	Easy
	5 Zealots	5 Zealots	Symmetric	
1c3s5z	1 Colossus	1 Colossus	Heterogeneous	Easy
	3 Stalkers	3 Stalkers	Symmetric	
	5 Zealots	5 Zealots		
5m_vs_6m	5 Marines	6 Marines	Homogeneous Asymmetric	hard
3s_vs_5z	3 Stalkers	5 Zealots	Homogeneous Asymmetric	hard
bane_vs_bane	4 Banelings	4 Banelings	Heterogeneous	hard
	20 Zerglings	20 Zerglings	Symmetric	
2c_vs_64zg	2 Colossi	64 Zerglings	Homogeneous	hard
			Asymmetric Large Action Space	
MMM2	1 Medivac	1 Medivac	Heterogeneous	Super Hard
	2 Marauders	3 Marauder	Asymmetric	
	7 Marines	8 Marines	Macro tactics	
27m_vs_30m	27 Marines	30 Marines	Homogeneous Asymmetric Massive Agents	Super Hard

Table B.1: Maps in different scenarios.

B.2 Hyperparameters

Hyperparameters were based on the PyMARL implementation and are listed in Table B.2. All experiments in this paper are run on Nvidia GeForce RTX 3090 graphics cards and Intel(R) Xeon(R) Platinum 8280 CPU. The epsilon annealing period (for epsilon-greedy exploration) is 50000 steps and in order to be fair, we set the ϵ of the high-level policy to be consistent with that of the low-level policy.

Name	Description	Value
	Learning rate	0.0005
	Type of optimizer	RMSProp
optim α	RMSProp param	0.99
optim ϵ	RMSProp param	0.00001
	How many episodes to update target networks	200
	Reduce global norm of gradients	10
	Batch size	32
	Capacity of replay buffer (in episodes)	5000
γ_h, γ_l	Discount factor	0.99
starting ϵ	Starting value for exploraton rate annealing	1
ending ϵ	Ending value for exploraton rate annealing	0.05
k	How many timesteps to execute the high-level policy	3
N	Number of macro actions	8

Table B.2: Hyperparameter settings.